Z. Phys. B - Condensed Matter 88, 205–212 (1992)

Condensed
Zeitschrift für Physik B Matter


# Re-entrant phase transitions of the Blume-Emery-Griffiths model

## I. Monte Carlo simulations on the simple cubic lattice

**Katsumi Kasono and Ikuo Ono**

Department of Physics, Tokyo Institute of Technology, Oh-Okayama, Meguro-ku, Tokyo 152, Japan

Received July 15, 1991; revised version February 18, 1992

We have investigated the spin-1 Ising model on the simple cubic lattice with bilinear, biquadratic interaction and anisotropic energy (BEG model). We have been specially interested in the case of antiferro biquadratic interaction, because the interaction will cause the competition with bilinear interaction and anisotropy. A two-sublattice ordering, so called the staggered quadrupole (SQ) phase, occurs as long as biquadratic interaction is negative large enough. We have obtained a full phase diagram in the whole interaction parameter space (for the positive bilinear interaction) by the Bethe approximation, and found several kinds of phase transitions, such as successive, re-entrant and double re-entrant transitions. These transitions are also confirmed by Monte Carlo simulations on simple cubic lattices.

### 1. Introduction

The Blume-Emery-Griffiths (BEG) model was originally proposed for the description of the phase transition in $He^3$-$He^4$ binary fluid [1], but later, many authors have investigated the BEG model as a spin system of rich phase transitions (a pioneer work is [2]). The partition function of the spin-1/2 Ising model with annealed site impurities in any dimension or any lattice can be also transformed into that of the BEG model [3]. The BEG Hamiltonian is given by

$$\mathscr{H} = -J_1 \sum_{\text{n.n.}} S_i S_j - J_2 \sum_{\text{n.n.}} S_i^2 S_j^2 - D \sum_i S_i^2, \tag{1}$$

where $S_i = 1, 0, 1$, the sum n.n. is over nearest neighbor pairs, and $D$ is the single-ion anisotropy energy. For special case of $J_2 = 0$, it is called the Blume-Capel model [4, 5]. Most of recent works on the phase transition of the BEG model have been devoted to the case of the antiferromagnetic biquadratic interaction ($J_2 < 0$) (for example, [6–8]), because it may be expected to give a rich phase diagram due to competition of interactions. As long as the biquadratic interaction $J_2$ is ferromagnetic ($J_2 > 0$), both of the ferromagnetic ($J_1 > 0$) and antiferromagnetic ($J_1 < 0$) phase are compatible with this interaction. On the other hand, when antiferromagnetic $J_2$ interaction and $D = 0$ are introduced, one spin of the interacting spin-pair is assumed to take 0 and the other spin prefers to take any of 1, 0, or $-1$ in the ground state. Thus the highly degenerate spin arrangement named as a staggered quadrupole (SQ) phase comes out [6, 7]. Here we will show that the BEG model exhibits various complicate phase transitions such as successive phase transition, re-entrant and double re-entrant phase transitions against the temperature. While the former analytical studies [8] were not enough to reveal these rich phase diagrams, because he overlooked a two-sublattice ordering. The ground state energy of the spin arrangement assumed by him is shown to be higher than our (SQ) phase in a certain range of parameter.

On the whole range of parameter space ($-\infty < J \equiv J_2/J_1 < +\infty$, $-\infty < D < +\infty$), we have obtained a phase diagram on the simple cubic lattice by the Bethe approximation (for square lattice, see [9]). The occurrence of re-entrant phase transitions on a simple cubic lattice is confirmed by Monte Carlo simulations.

The article is organized as follows. In Sect. 2 we investigate the spin arrangements of the two-sublattice for the ground state. In Sect. 3 their phase diagram is obtained by the Bethe approximation. The results of Monte Carlo simulations on simple cubic lattices are given in Sect. 4. Final Sect. 5 is devoted to a summary.

### 2. Definition of phases

At first, we consider the spin arrangements in the ground state of the BEG model in the case of $J_1 > 0$. As long as the two-sublattice ordering on the bipartite lattice is concerned, we introduce following three arrangements. We denote here $(S_i, S_j)$ as the spin state on the $A$ and $B$ sublattice.

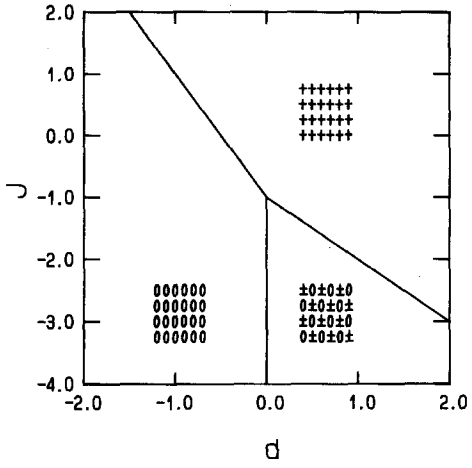


**Fig. 1.** The phase diagram ($d-J$ plane) and the spin arrangements in the ground state of the BEG model on a hyper-cubic lattice

*Case 1, perfect 0 ordering.* Both $S_i$ and $S_j$ take the value 0.
*Case 2, ferromagnetic ordering.* $(S_i, S_j)$ takes $(1, 1)$ or $(-1, -1)$ and it has trivial double degeneracy.
*Case 3, staggered quadrupole ordering.* $(S_i, S_j)$ takes either $(0, 1)$ or $(0, -1)$ randomly, so its residual entropy becomes $\frac{1}{2}\ln 2$ per spin.

The ground state enery $E_g$ depends on the parameter $J \equiv J_2/J_1, d \equiv D/zJ_1$ ($z$ is the coordination number). The phase diagram of the ground state is shown in Fig. 1 as a function of $J$ and $d$ and their ground state energy $E_g$ is as follows.

1. $E_g = 0$ $\quad d \leqq 0$ and $J \leqq -1-2d$
2. $E_g = \frac{1}{2}NzJ_1(-1-J-2d)$ $\quad J \geqq -1-d$ and $J \geqq -1-2d$
3. $E_g = \frac{1}{2}NzJ_1(-d)$ $\quad d \geqq 0$ and $J \leqq -1-d$.

Let us introduce the four order parameters describing the ordering for the two-sublattice $(A, B)$; $m_A = \langle S_A \rangle$, $q_A = \langle S_A^2 \rangle$, $m_B = \langle S_B \rangle$, $q_B = \langle S_B^2 \rangle$ and define the next five phases at non zero temperature.

*i. One-sublattice phases*
0. spherical phase (disordered phase) (S)

$m_A = m_B = 0$ and $q_A = q_B = 2/3$

1. quadrupole phase (Q)

$m_A = m_B = 0$ and $q_A = q_B \neq 2/3$

2. ferromagnetic phase (F)

$m_A = m_B \neq 0$

*ii. Two-sublattice phases*
3. staggered quadrupole phase (SQ)

$m_A = m_B = 0$ and $q_A \neq q_B$

4. ferrimagnetic phase (FR)

$m_A \neq m_B$ and $q_A \neq q_B$.

Here these order parameters are bounded to be $|m_A| \leqq q_A \leqq 1$ and $|m_B| \leqq q_B \leqq 1$. In the highest temperature limit, $S_i$ takes either 0, 1 or $-1$ in the complete random way. Thus we have a spherical (S) phase when order parameters become $q_A = q_B = 2/3$ and $m_A = m_B = 0$. The order parameter $q$ is deviated gradually from 2/3 when the temperature is decreased. The perfect 0 phase in the ground state belongs to the (Q) phase, because its order parameters are given by $q_A = q_B = 0$ and $m_A = m_B = 0$. When $J$ is positive large enough and $D$ is also positive, we have the ferromagnetic (F) phase in the lowest temperature. The (FR) phase, which was referred in [2], have never appeared in the whole temperature range.

When $J_1 < 0$, the whole phase diagram is unchanged except the (F) phase is replaced by antiferro (AF) phase, because the Hamiltonian (1) is conserved under simultaneously changing $J_1 \to -J_1$ and the inversion of every spin in one sublattice. Hereafter the exchange parameter $J_1$ can be assumed to be positive without loss of generality.

## 3. The Bethe approximation

To obtain the phase diagram we have applied the Bethe approximation [10] to the BEG Hamiltonian. For convenience, we introduce the magnetic field $H$. The one-site effective Hamiltonian $\mathscr{H}_A^{(1)}$, $\mathscr{H}_B^{(1)}$ of $A$ and $B$ sublattice are assumed to be written by

$$\mathscr{H}_A^{(1)} = -zH_A S_A - zD_A S_A^2 - HS_A - DS_A^2 \tag{2}$$

$$\mathscr{H}_B^{(1)} = -zH_B S_B - zD_B S_B^2 - HS_B - DS_B^2, \tag{3}$$

and the two-site effective Hamiltonian $\mathscr{H}_{A,B}^{(2)}$

$$\begin{aligned}\mathscr{H}_{A,B}^{(2)} = & -J_1 S_A S_B - J_2 S_A^2 S_B^2 - HS_A - HS_B \\ & - DS_A^2 - DS_B^2 \\ & - (z-1)H_A S_A - (z-1)H_B S_B \\ & - (z-1)D_A S_A^2 - (z-1)D_B S_B^2,\end{aligned} \tag{4}$$

where the parameters $H_A, H_B, D_A$ and $D_B$ are to be determined from the condition of minimizing the free energy. The free energy $F$ corresponding to the Bethe approximation can be given as follows [11].

$$\begin{aligned}-\beta F = & \sum_i \ln \mathrm{Tr}\, \rho_i^{(1)} \\ & + \sum_{\text{n.n.}} [\ln \mathrm{Tr}\, \rho_{i,j}^{(2)} - \ln \mathrm{Tr}\, \rho_i^{(1)} - \ln \mathrm{Tr}\, \rho_j^{(1)}]\end{aligned} \tag{5}$$

$$\begin{aligned}= & \tfrac{1}{2} zN \ln \mathrm{Tr}\, \rho_{A,B}^{(2)} \\ & + \tfrac{1}{2}(1-z)N[\ln \mathrm{Tr}\, \rho_A^{(1)} + \ln \mathrm{Tr}\, \rho_B^{(1)}],\end{aligned} \tag{6}$$

where the density matrices $\rho_A^{(1)}, \rho_B^{(1)}$ and $\rho_{AB}^{(2)}$ are given by

$$\rho_A^{(1)} = \exp(-\beta \mathscr{H}_A^{(1)}), \tag{7}$$

$$\rho_B^{(1)} = \exp(-\beta \mathscr{H}_B^{(1)}), \tag{8}$$

$$\rho_{A,B}^{(2)} = \exp(-\beta \mathscr{H}_{A,B}^{(2)}). \tag{9}$$

Differenciating the free energy function with respect to $H_A, H_B, D_A$ and $D_B$, we have

$$\frac{\partial F}{\partial H_A} = \frac{\partial F}{\partial H_B} = \frac{\partial F}{\partial D_A} = \frac{\partial F}{\partial D_B} = 0. \tag{10}$$

The explicit forms of (10) are

$$\frac{X(H_A, H_B, D_A, D_B)}{Z^{(2)}(H_A, H_B, D_A, D_B)} = \frac{2\exp\{\beta(D+zD_A)\}\sinh\{\beta(H+zH_A)\}}{1+2\exp\{\beta(D+zD_A)\}\cosh\{\beta(H+zH_A)\}} = m_A, \tag{11}$$

$$\frac{X(H_B, H_A, D_A, D_B)}{Z^{(2)}(H_A, H_B, D_A, D_B)} = \frac{2\exp\{\beta(D+zD_B)\}\sinh\{\beta(H+zH_B)\}}{1+2\exp\{\beta(D+zD_B)\}\cosh\{\beta(H+zH_B)\}} = m_B, \tag{12}$$

$$\frac{Y(H_A, H_B, D_A, D_B)}{Z^{(2)}(H_A, H_B, D_A, D_B)} = \frac{2\exp\{\beta(D+zD_A)\}\cosh\{\beta(H+zH_A)\}}{1+2\exp\{\beta(D+zD_A)\}\cosh\{\beta(H+zH_A)\}} = q_A, \tag{13}$$

$$\frac{Y(H_B, H_A, D_A, D_B)}{Z^{(2)}(H_A, H_B, D_A, D_B)} = \frac{2\exp\{\beta(D+zD_B)\}\cosh\{\beta(H+zH_B)\}}{1+2\exp\{\beta(D+zD_B)\}\cosh\{\beta(H+zH_B)\}} = q_B, \tag{14}$$

where

$$\begin{aligned} X(H_1, H_2, D_1, D_2) &= 2\exp[\beta\{D+(z-1)D_1\}] \\ &\times \sinh[\beta\{H+(z-1)H_1\} \\ &+ 2\exp[\beta\{J_2+2D+(z-1)(D_1+D_2)\}] \\ &\times\{\exp(\beta J_1)\sinh[\beta\{2H+(z-1)(H_1+H_2)\}] \\ &+ \exp(-\beta J_1)\sinh[\beta\{(z-1)(H_1-H_2)\}]\}, \end{aligned} \tag{15}$$

$$\begin{aligned} Y(H_1, H_2, D_1, D_2) &= 2\exp[\beta\{D+(z-1)D_1\}] \\ &\times \cosh[\beta\{H+(z-1)H_1\}] \\ &+ 2\exp[\beta\{J_2+2D+(z-1)(D_1+D_2)\}] \\ &\times\{\exp(\beta J_1)\cosh[\beta\{2H+(z-1)(H_1+H_2)\}] \\ &+ \exp(-\beta J_1)\cosh[\beta\{(z-1)(H_1-H_2)\}]\}, \end{aligned} \tag{16}$$

$$\begin{aligned} Z^{(2)}(H_1, H_2, D_1, D_2) &= 1+2\exp[\beta\{D+(z-1)D_1\}] \\ &\times \cosh[\beta\{H+(z-1)H_1\}] \\ &+ 2\exp[\beta\{D+(z-1)D_2\}]\cosh[\beta\{H+(z-1)H_2\}] \\ &+ 2\exp[\beta\{J_2+2D+(z-1)(D_1+D_2)\}] \\ &\times\{\exp(\beta J_1)\cosh[\beta\{2H+(z-1)(H_1+H_2)\}] \\ &+ \exp(-\beta J_1)\cosh[\beta\{(z-1)(H_1-H_2)\}]\}. \end{aligned} \tag{17}$$

When $H=D=0$, the self-consistent equations (11–14) include, as expected, the solution $H_A=H_B=0$ and $D_A=D_B=0$ in the highest limiting temperature. This represents the spherical phase where the same probabilities of distribution appear for $S=-1$, 0 and 1. In the (Q) phase, the order parameter $q(=q_A=q_B)$ is always dependent on the temperature. Hereafter we try to find the ordered phase under the condition $H=0$ and $D\neq 0$. We consider first a one-sublattice phase where $q_A=q_B=q$ and $m_A=m_B=m$. The critical frontier for vanishing the (F) phase is determined by setting $m\to+0$. On the other hand the critical frontier for vanishing the (SQ) phase is given by $|q_A-q_B|\to 0$ under the condition $m_A=m_B=0$. These conditions lead the relation among $J$, $d$, and $T$. In order to avoid the quasistable solutions, we also have compared the free energies corresponding the (Q), (F) and (SQ) phases each other.

The phase diagrams are shown separately in Fig. 2a for $d=1.0$, 0.5, 0.0, $-0.5$ and $-1.0$ and in Fig. 2b for $d=0.0$, $-0.05$, $-0.1$, $-0.2$, $-0.25$ and $-0.4$. One can see the general aspect of the phase transitions of the BEG model. At the low temperature the (F) phase generally appears when $J(=J_2/J_1)$ is positive and large enough, while the (SQ) phase appears when $J$ is negative and large absolute value. When $d=0$, these two phases meet at the point $J=-1$ and $T=0$. As $d$ increases from zero the area of the (F) and the (SQ) phases expand, and thus they look like overlapping each other. In this region the first-order phase transition occurs between the (F) and (SQ) phases.

In the case of $d<0$ the phase diagram is, as shown in Fig. 2b, turned to be more complicated. The areas of the (F) and (SQ) phases become to separate each other and there happens no phase transition in the intermediate $J$. Moreover a tricritical point appears on the critical frontier of the (F) phase [12]. Specially when $d$ is small absolute value, the re-entrant transition, that is, (Q)→(F)→(Q) may occur for the restricted $J$. As for the (SQ) phase one can see the re-entrant transition appears more generally when $d<0$ and $J<0$. This should not be surprised, because the ground state is the perfect 0 ordering, and its symmetry belongs to the (Q) phase.

Other complex phase transitions are found as described in following.

*(a)* Successive transition (Q)→(F)→(SQ) when $d>0$ and $J$ is slightly smaller than $-1-d$.

The transition from the (F) to the (SQ) phase is of first-order.

It is seen from Fig. 2b that four types of re-entrant transitions occur in the vicinity of small $d$ as follows.

*(b)* Re-entrant transition (Q)→(SQ)→(Q) when $d=-0.05$, $-0.1$ or $-0.2$ and $J<-1$.

*(c)* Re-entrant transition (Q)→(F)→(Q) when $d=-0.05$, $-0.1$, $-0.2$ or $-0.25$ and $J$ is slightly smaller than $-1-2d$.

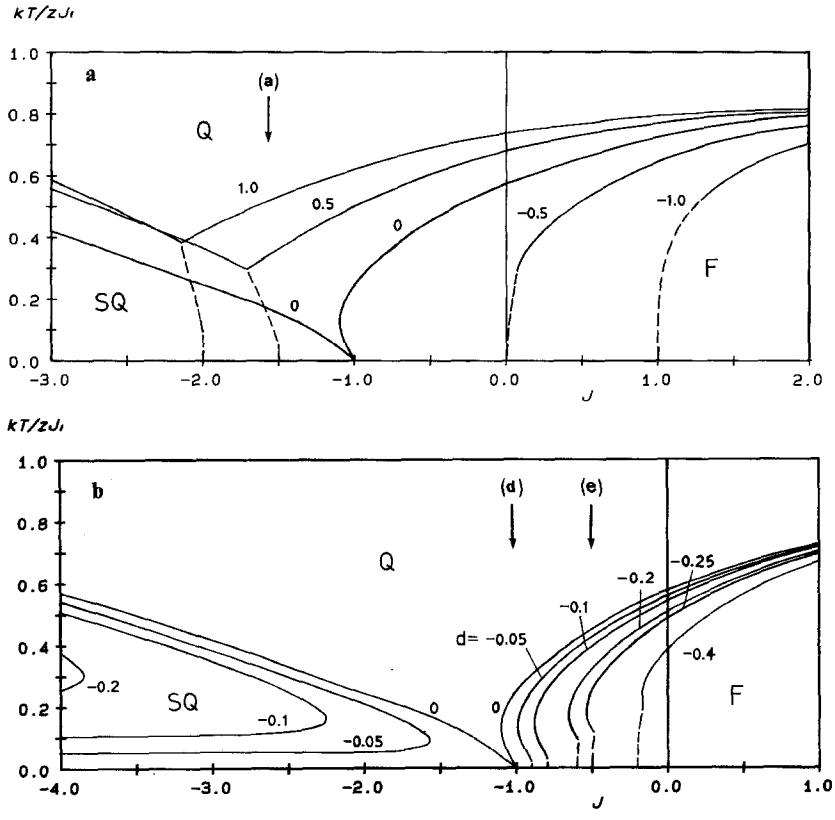


**Fig. 2a, b.** The phase diagram for the several values of $d$ is plotted in $J \equiv J_2/J_1$ and the reduced temperature plane. **a** $d=1.0$, 0.5, 0.0, $-0.5$, $-1.0$ and **b** $d=0.0$, $-0.05$, $-0.1$, $-0.2$, $-0.25$, $-0.4$. The right-side lines indicate the (Q)→(F) phase transition, and left-hand lines the (Q)→(SQ) phase transition. When $d>0$ both phases overlap each other, and the first-order (F)→(SQ) transition appears, a tricritical point appears on the critical frontier of the (F) phase. Here the solid lines and the broken lines indicate the continuous and first-order transition, respectively

*(d)* Re-entrant and successive transition (Q)→(F)→(Q)→(SQ) when $d=0$ and $-1.05 < J < -1.0$.
*(e)* Double re-entrant transition (Q)→(F)→(Q)→(F) when $-0.2 < d < -0.3$ and $J$ is slightly larger than $-1-2d$. All re-entrant transitions are found to be continuous except the lower transitions (Q)→(F) in the case *(e)*.

Here cases *(b)* and *(c)* have been obtained by various methods in former papers. For instance, *(b)*: mean field approximation [1, 2], Monte Carlo method [6], [7] ($J_1=0$), *(c)*: the Bethe approximation, renormalization group method, Monte Carlo method (these are one-sublattice treatments and $D=0$ see [13]). For *(a)*, Blume et al. [1] and Chen et al. [2] did not show to appear the successive transition although they took into account the two-sublattice ordering. In order to confirm the appearance of the above-mentioned complex phase transitions, we have performed Monte Carlo simulations. We will refer to *(a), (d), (e)* later in this paper.

## 4. The Monte Carlo simulation and thermal properties in the ordered states

Simulations were executed by the Metropolis algorithm on $N(=L\times L\times L)$ sited simple cubic lattices with a periodic boundary condition in all lattice directions, where $L$ is the linear size of the system. Thermal quantities are estimated after discarding the first 10 000 Monte Carlo steps (MCS), and typical observation times are over 100 000 ~ 200 000 MCS. We use the binning method for error estimates [14]. The supercomputer HITAC S-820/

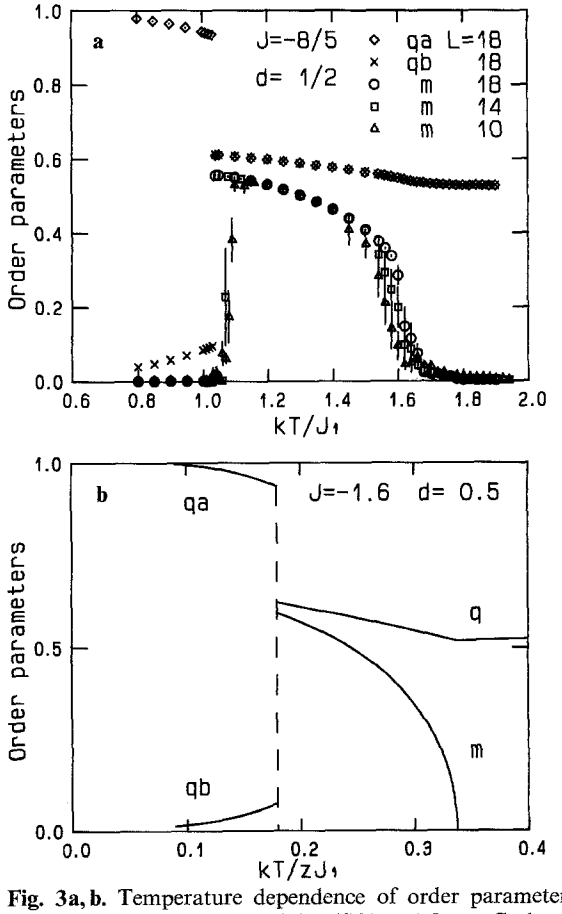


**Fig. 3a, b.** Temperature dependence of order parameters for the successive transition (Q)→(F)→(SQ); **a** Monte Carlo simulation on the simple-cubic lattice of $L\times L\times L$ ($L=10$, 14, 18), **b** the Bethe approximation

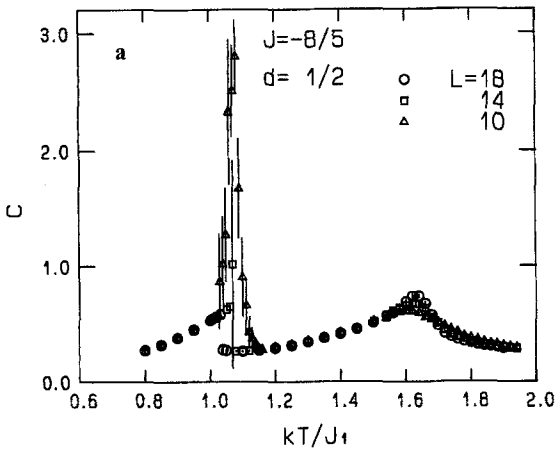


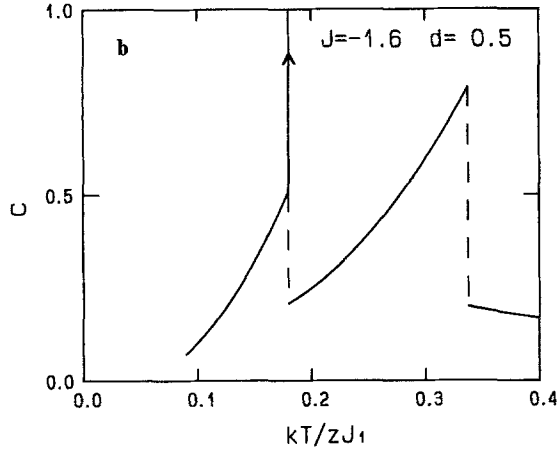


**Fig. 4a, b.** Temperature dependence of specific heat for the successive transition (Q)→(F)→(SQ) ($L=10$, 14, 18)

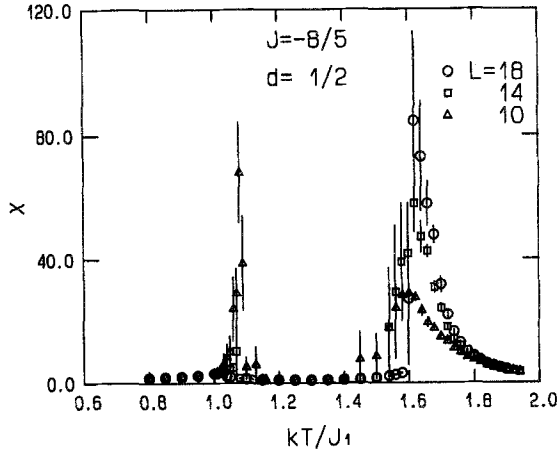


**Fig. 5.** Temperature dependence of susceptibility for the successive transition (Q)→(F)→(SQ) ($L=10$, 14, 18)

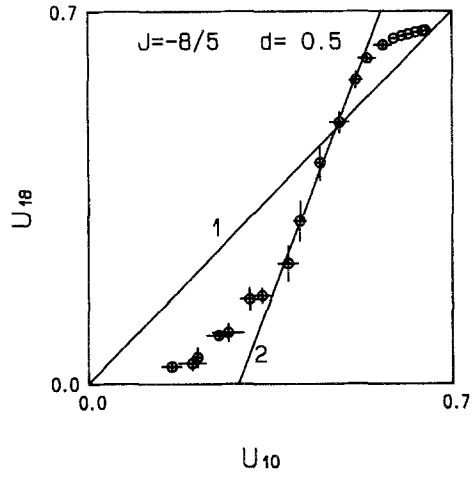


**Fig. 6.** Fourth-order cumulant $U_{10}$ versus $U_{18}$ obtained by Monte Carlo simulations around the transition (Q)→(F). If $L$ is large enough, the transition temperature or fixed point is drawn when the size dependency in $U$'s disappears i.e. $U_{10}=U_{18}$. The critical exponent $\nu=0.63$ (line 2) $\pm 0.05$ and $T_C=1.65\pm 0.01$ are estimated

880 at the Institute for Molecular Science has ability of updating about $2\times 10^7$ spins per s. The simulations are performed for the case of special values of parameters with which above-mentioned interesting phase transitions are expected to appear.

### *4.1. Successive transition* (Q)→(F)→(SQ)

Here we set the interaction parameters to be $J=-8/5$, $d=1/2$ which are shown as an arrow (a) in Fig. 2a. Order parameters obtained by the Monte Carlo method (MC) are shown in Fig. 3a, and those by the Bethe approximation (BA) are shown in Fig. 3b. Specific heat by MC and BA are in Fig. 4a and b respectively.

As seen from Figs. 3a and 4a, the lower phase transition (F)→(SQ) should be assigned as a first-order transition because the jump of order parameters appear and the specific heat has very sharp peak. The specific heat by BA involves a latent heat shown as a delta function singularity at this transition in Fig. 4b. If the transition is the second-order, the specific heat by BA represents the finite jump at the transition temperature. The estimation of this first-order transition temperature by BA is proved to be 1.08, which is near to 1.05 obtained by MC. The susceptibility obtained by MC, as shown in Fig. 5, looks to diverge sharply when $L=10$ at the lower transition temperature, but not to diverge when $L=14$ and 18. The reason may be attribute to the region of transition where the susceptibility becomes divergent must shrink rapidly to a point of the transition temperature when the lattice size $L$ approaches infinity in the case of the first-order transition.

The higher transition (Q)→(F) looks a continuous transition, because the magnetization appears continuously and the order parameter $q$ has a weak kink at the transition temperature, as seen from Fig. 3a. The estimated transition temperature from MC is given by 1.65, which should be compared to 2.02 estimated from BA. This ferromagnetic transition accompanies the strong peak of susceptibility, as shown in Fig. 5. While the specific heat is found to have a small peak as shown in Fig. 4a.

We have attempted further to estimate the more accurate critical point $T_C$ and critical exponent $\nu$ by use of

Binder's fourth-order cumulant $U_L$, which is defined by $U_L=(\langle M^4\rangle-3\langle M^2\rangle^2)/\langle M^2\rangle^2$ [15], where $M=\sum_i S_i$ and $L$ denotes the linear size of the lattice. We plot $U_{18}$ versus $U_{10}$ in Fig. 6 for several temperatures. The temperature where $U_L(T)=U_{L'}(T)$ $(L, L'\gg 1)$ can be identified with $T_C$ and the gradient of the curve of MC data at $T_C$ gives $(L'/L)^{1/\nu}$. We have concluded that $T_C=1.65\pm 0.01$ and $\nu=0.63\pm 0.05$. This result shows the transition belongs to a three dimensional Ising class.

### 4.2. *Re-entrant transition* (Q)→(F)→(Q)→(SQ)

We have used the values $J=-31/30$ and $d=0$ in MC, which are shown as an arrow (d) in Fig. 2b and used values $J=-1.05$, $d=0$ in BA. Since $D=0$, only $J_1$ and $J_2$ are competing. This coupling parameter is near to the triple point at the absolute zero as seen in Fig. 1. The order parameters and specific heats are plotted in Figs. 7a, b and 8a, b respectively. Here the thermal quantities are averaged over 30 000 ~ 50 000 MCS.

The lower transition (Q)→(SQ) is proved to occur at extremely low temperature and to be of continuous transition from the temperature dependence of the order parameters $q_A$ and $q_B$. A sharp peak of specific heat by MC, as seen in Fig. 8a, is compatible with the second-order transition.

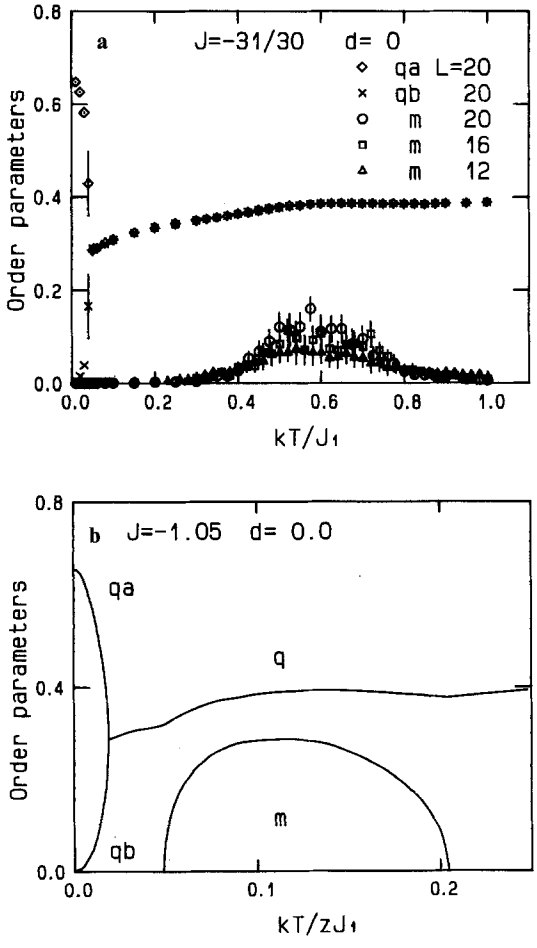


**Fig. 7a, b.** Temperature dependence of order parameters for the re-entrant transition (Q)→(F)→(Q)→(SQ); **a** Monte Carlo simulation on the simple-cubic lattice of $L\times L\times L$ $(L=12, 16, 20)$, **b** the Bethe approximation

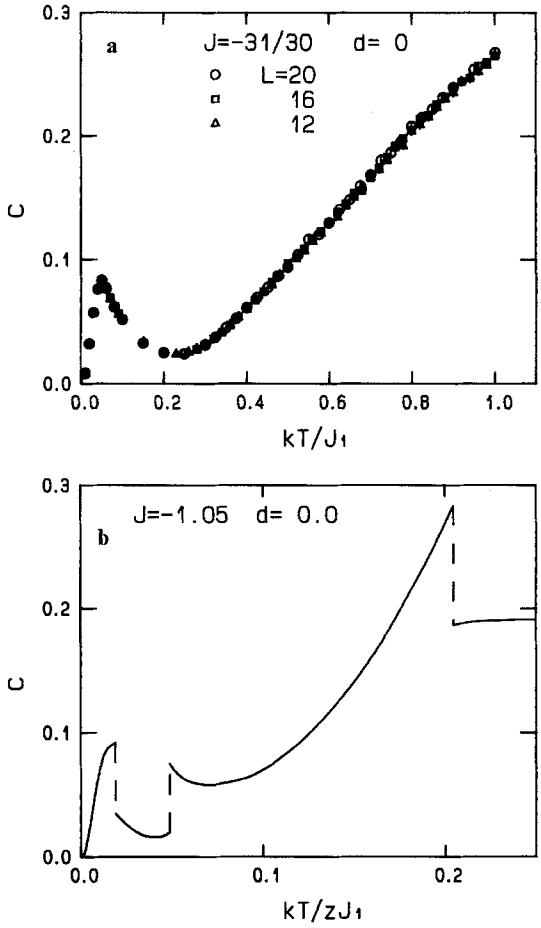


**Fig. 8a, b.** Temperature dependence of specific heat for the re-entrant transition (Q)→(F)→(Q)→(SQ); **a** Monte Carlo simulation $(L=12, 16, 20)$, **b** the Bethe approximation

The magnetization of the (F) phase in the intermediate temperature seems to be very weak as seen from Fig. 7a. Nevertheless the (F) phase may be concluded to exist, since its magnetization $m$ increases when the lattice size increases. The specific heat at the both transitions (Q)→(F) and (F)→(Q) have no sign of singularity. This behavior is found in the next double re-entrant phase transition in Fig. 10a as well. On the other hand the susceptibility on MC indicates the existence of the singularities which is not shown here. Lushnikov studied the two and three dimensional spin-1/2 Ising model with annealed site and bond impurities [3, 16], and concluded a third-order transition, because the temperature-derivative of the specific heat has anomaly at the transition temperature. Thus these transitions are possible to be of third-order, but our MC data on specific heat have not enough to answer whether the (Q)→(F) transition is a second or third-order transition.

### 4.3. *Double re-entrant transition* (Q)→(F)→(Q)→(F)

Here we have used $J=-1/2$, $d=-89/360$ in MC, which is shown as an arrow (e) in Fig. 2b and $J=-0.325$,

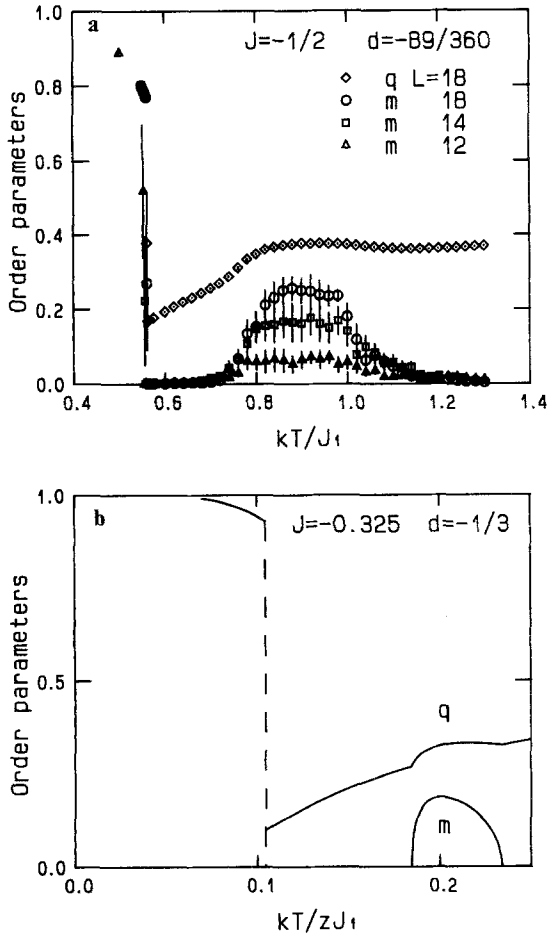


**Fig. 9a, b.** Temperature dependence of order parameters for the double re-entrant transition (Q)→(F)→(Q)→(F); **a** Monte Carlo simulation ($L=12$, 14, 18), **b** the Bethe approximation

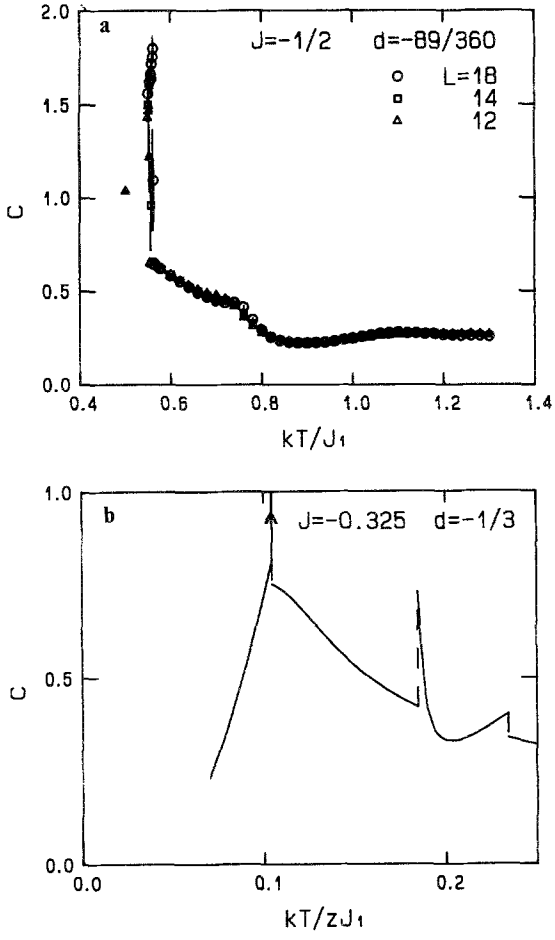


**Fig. 10a, b.** Temperature dependence of specific heat for the double re-entrant transition (Q)→(F)→(Q)→(F); **a** Monte Carlo simulation ($L=12$, 14, 18), **b** the Bethe approximation

$d=1/3$ in BA. The order parameters obtained from MC and BA are shown comparatively in Fig. 9a, b. Here the initial state in the simulation is set to be all $S_i=1$ at the lowest temperature and then temperature is grown up. The phase transition between the lowest (F) phase and the intermediate (Q) phase exhibits a jump of order parameter at $T=0.56$, as shwon in Fig. 9a, and a sharp peak of specific heat is found at the same temperature as shwon in Fig. 10a. This result is compatible with the first-order transition expected by BA shown in Fig. 10b.

The magnetization in the (F) phase at the intermediate temperature shows the considerable size-dependency in contrast to the lowest (F) phase. This (F) phase involves the strong fluctuation even in the ordered state due to the competition of interaction parameters. The specific heat in the re-entrant (F) phase, as shown in Fig. 10a, has a kink at $T=0.76$, but it has scarcely singularity at the higher transition temperatures.

We have also attempted to determine the critical point in more precisely by use of the size dependence of fourth-order cumulant $U_L$. The critical point is shown in Fig. 11 and $T_C=0.76$ and $1.10(\pm 0.02)$ are obtained. The fourth-cumulant suggests that the exponents $\nu$ for both of these transitions are the same value obtained in 4.1.

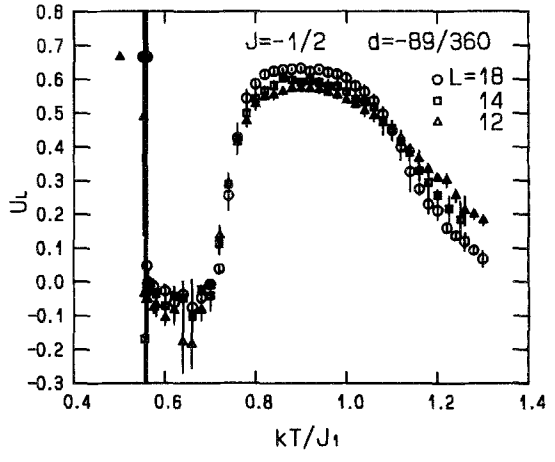


**Fig. 11.** Temperature dependence of fourth-order cumulant $U_L$ for the double re-entrant transition (Q)→(F)→(Q)→(F) by Monte Carlo simulation ($L=12$, 14, 18). $T_C=0.76$ and $1.10(\pm 0.02)$

## 5. Summary

The phase diagram of the Blume-Emery-Griffiths model has obtained in the full $J_1-J_2-D$ parameter space by the Bethe approximation. We have found several re-en-

trant phase transitions and first-order successive transition depending on interaction parameters. The occurrence of the re-entrant phases are confirmed by Monte Carlo simulations on simple cubic lattices. It should be noted that the specific heat of re-entrant phase transition shows the gentle behavior.

This study was carried out under the Institute of Statistical Mathematics Cooperative Research Program (91-ISM·CRP-37). We have partially used the HITAC S-820/80 at the Institute for Molecular Science.

## References

1. Blume, M., Emery, V.J., Griffiths, R.B.: Phys. Rev. A**4**, 1071 (1971)
2. Chen, H.H., Levy, P.H.: Phys. Rev. B**7**, 4267 (1973)
3. Lushnikov, A.A.: Phys. Lett. A**40**, 303 (1972)
4. Blume, M.: Phys. Rev. **141**, 517 (1966)
5. Capel, H.W.: Physica **32**, 966 (1966)
6. Wang, Y.L., Wentworth, C.: J. Appl. Phys. **61**, 4411 (1987)
7. Ono, I.: J. Phys. (Paris) C**8**, 1541 (1988)
8. Kaneyoshi, T.: J. Phys. Soc. Jpn. **56**, 4199 (1987)
9. Tanaka, M., Kawabe, T.: J. Phys. Soc. Jpn. **54**, 2194 (1985)
10. Oguchi, T., Ono, I.: J. Phys. Soc. Jpn. **21**, 2178 (1966)
11. Morita, T.: Physica A**98**, 566 (1979)
12. Lawrie, I.D., Sarbach, S.: In: Phase transition and critical phenomena. Domb, C., Lebowitz, J.L. (eds.), Vol. 9. Berlin, Heidelberg, New York: Springer 1983
13. de Alcantara Bonfim, O.F., Obcemea, C.H.: Z. Phys. B - Condensed Matter **64**, 469 (1986)
14. Landau, D.P.: Phys. Rev. B**13**, 2997 (1975)
15. Binder, K.: Z. Phys. B - Condensed Matter **43**, 119 (1981)
16. Lushnikov, A.A.: Sov. Phys. JETP **29**, 120 (1969)